water

MDPI

Article

The Synthesis of PbS NPs and Biosorption of Pb(II) by *Shinella Zoogloeoides* PQ7 in Aqueous Conditions

Wei Zhang and Yili Huang *

Zhejiang Provincial Key Laboratory of Organic Pollution Process and Control, Department of Environmental Science, College of Environmental and Resource Sciences, Zhejiang University, Hang Zhou 310000, China; 21714006@zju.edu.cn

* Correspondence: yilihuang@zju.edu.cn; Tel./Fax: +86-571-88982592

Received: 6 May 2020; Accepted: 27 May 2020; Published: 21 July 2020

Abstract: Increasing heavy metal pollution in water continues to endanger human health. The genus *Shinella* has potential for heavy metal bioremediation but has rarely been studied. In this study, we report that *Shinella zoogloeoides* PQ7 turns black in the presence of lead ions. Transmission electron microscopy (TEM), Scanning electron microscopy–energy dispersive X-ray spectroscopy (SEM–EDS), X-ray photoelectron spectroscopy (XPS) and X-ray diffraction (XRD) indicated that PbS nanoparticles (NPs) were synthesized by PQ7. Moreover, PQ7 was used as a biosorbent to remove Pb(II) from aqueous solutions. Biosorption performance was evaluated in terms of contact time, pH, biomass dosage and initial Pb(II) concentration. The equilibrium and kinetic data were consistent with the Freundlich isotherm model (R^2 = 0.986) and pseudo-second-order model (R^2 = 0.977), respectively. The maximum (q_{max}) Pb(II) adsorption reached 222.22 mg/g, which was higher than that of other bacteria reported in previous literature. SEM–EDS, XRD and Fourier transform infrared (FTIR) analyses also confirmed the adsorption of Pb(II) by the PQ7 cells. In conclusion, PQ7 is a promising strain in removing and recovering Pb(II) from wastewater.

Keywords: *Shinella zoogloeoides* PQ7; PbS nanoparticles; biosorption; lead(II); bioremediation

1. Introduction

Heavy metals are among the most concerning environmental pollutants because of their toxicity and tendency to accumulate in the environment [1,2]. Lead(Pb) is one of most concerning heavy metals [3]. Many studies have reported that Pb(II) can damage human tissues and affect human health. Pb(II) can be toxic by interacting with calcium(II) to replace it in bones or combining with zinc(II) in haem enzymes and metallothioneins [4,5]. Because of these serious effects, it is essential to remove and recover lead ions from wastewater and the environment.

Many methods, including ionic exchange, chemical precipitation and electrolysis, have been used for the removal of lead ions. However, these methods are often not friendly to the environments [6]. Microbes based biotechnology has shown promising future in the bioremediation of heavy metals because of their low cost and high efficiency [2]. Some bacteria can not only survive in the presence of Pb(II) but also form valuable lead compounds. For example, *Streptomyces* sp. and *Pseudomonas vesicularis* have been reported to produce red and red–brown pigments Pb_3O_4 [7]. $Pb_9(PO_4)_6$, $PbSO_4$, PbS, $Pb_5(PO_4)_3Cl$, and $PbHPO_4$ are also synthesized by lead-resistant bacteria [8–10]. Some bacteria, yeasts and fungi have been reported to synthesize PbS nanoparticles (NPs) [11–15]. PbS is a semiconductor material based on heavy metals. When synthesized at the nanoscale, its chemical, electrical, optical and magnetic properties are superior to those of same-volume semiconductor materials [16]. Compared to physical and chemical, using microorganisms to synthesize PbS nanoparticles is the most economical

method [11]. Thus, it is meaningful to find lead-resistant bacteria that not only are efficient absorbents but also form useful lead compounds.

Quite a few species in the genus *Shinella* had been reported to degrade organic pollutants, such as nicotine, pyridine and polycyclic aromatic hydrocarbons [17–20]. However, very few studies have explored their bioremediation in terms of heavy metals. *Shinella zoogloeoides* PQ7 was isolated from contaminated soil [17]. It can resist quite a few heavy metals, such as zinc(II), copper(II), lead(II) and chromium(IV), and turn black in the presence of lead ions. This study was carried out to explore the reason for this color change in the presence of lead ions and the adsorption of Pb(II). To this end, transmission electron microscopy (TEM), scanning electron microscopy–energy dispersive X-ray spectroscopy (SEM–EDS), X-ray photoelectron spectroscopy (XPS) and X-ray diffraction (XRD) were employed to characterize the black materials. Different experimental factors, kinetic models and isotherm models were used to investigate the adsorption behavior.

2. Materials and Methods

2.1. Bacterial Strain and Culture Conditions

Shinella zoogloeoides PQ7 was obtained from our lab collection in 2013 [17]. It was grown in Luria-Bertani (LB) medium (tryptone 10 g/L, sodium chloride 10 g/L, yeast extract 5 g/L) at 30 °C with 200 rpm shaking speed.

2.2. Growth of Shinella Zoogloeoides PQ7 in the Presence of Lead Ions

One milliliter seed culture of PQ7 (OD_{600} = 1) was inoculated into 100 mL LB liquid medium with lead ions (5 mM). Then, the cultures were cultivated at 30 °C with a shaking speed of 200 rpm. The growth of the cells was monitored daily. LB medium without Pb(II) served as controls. Each experiment was carried out in triplicate.

2.3. Transmission Electron Microscopy (TEM) and Scanning Electron Microscopy–Energy Dispersive X-ray Spectroscopy (SEM–EDS) Analysis

After four days cultivation, when *Shinella zoogloeoides* PQ7 turned black in the presence of Pb(II) ions, the black bacterial cells and control cells were collected by centrifuging at 10,000 rpm for 15 min and washed 3 times with sterile distilled water for the next steps.

The samples were fixed in 2.5% glutaraldehyde overnight at 4 °C and then washed three times with 0.1 M phosphate buffer. After fixation with osmium acid for 2 h, the bacteria were gradually dehydrated in a gradient series of solutions containing different ethanol concentrations. Then, samples were prepared following standard procedures according to a previous study [1]. Finally, the bacteria were analyzed by SEM–EDS (SU-8010, Hitachi, Tokyo, Japan).

After being dried in a graded sequence of ethanol, the samples for TEM were placed in the mixture of alcohol and isoamylacetate (*v*:*v* = 1:1) for 0.5 h, and subsequently transferred to isoamylacetate for 12 h. After that, the samples were washed and dried in liquid CO_2 (Hitachi Model HCP-C criticalpoint dryer). Desiccated samples were coated with gold-palladium (Hitachi Model E-1010 ion sputter) and then observed in TEM (Hitachi H7650) [1].

2.4. X-ray Diffraction (XRD) and X-ray Photoelectron Spectroscopy (XPS) Analysis

The black cells were characterized by XRD (D8 Advance, Germany) and XPS (K-Alpha+, Thermo Scientific, Waltham, MA, USA) to analyze the black materials formed by *Shinella zoogloeoides* PQ7. The samples were treated with a series of gradient concentrations of alcohol and acetone to dehydrate them. After being freeze-dried, the dried materials were mashed and characterized by XRD and XPS.

2.5. Biosorption Experiments

One milliliter seed culture of PQ7 (OD_{600} = 1) was inoculated into 100 mL LB medium at 30 °C with 200 rpm shaking speed until the stationary phase was reached. The cells were collected by centrifugation at 10,000 rpm for 15 min and washed three times with deionized water [21]. Then, the samples were used for biosorption experiments.

To fully evaluate the adsorption characteristics of lead ions by the strain, several parameters, such as pH, contact time, biomass dosage and initial Pb(II) concentration, were changed. The pH of the 100 mL lead solution was changed using 0.1 M NaOH or HCl solutions. Dry bacterial samples (0.1 g) were suspended in 100 mL lead solutions and then agitated at 30 °C with 200 rpm shaking speed. At certain times, the residual Pb(II) was detected by inductively coupled plasma–mass spectrometry (ICP–MS, 7700X, Agilent, Santa Clare, CA, USA). All biosorption experiments had three biological replicates, and the mean values were also calculated.

Equations (1) and (2) were used to determine the biosorption rate and capacity of lead ions [22]:

$$\text{Biosorption rates } (\%) = \frac{C_0 - C_e}{C_0} \times 100 \quad (1)$$

$$q_e = \frac{C_0 - C_e}{M} \quad (2)$$

where C_0 and C_e (mg/L) represent the beginning and end concentrations of lead ions, respectively; q_e (mg/g) is the biosorption capacity at equilibrium; and M (g/L) corresponds to the biomass concentration.

2.6. Kinetic and Biosorption Isotherm Studies

The adsorption reaction rate and capacity of an adsorbent could be described by adsorption kinetics. In this study, pseudo-first-order and pseudo-second-order Equations (3) and (4) were used to investigate the kinetics of Pb^{2+} biosorption [23,24]:

$$q_t = q_{e1}(1 - \exp(-k_1 t)) \quad (3)$$

$$q_t = \frac{q_{e2}^2 K_2 t}{1 + q_{e2} K_2 t} \quad (4)$$

where q_t (mg/g) is the concentration of Pb(II) adsorbed at time t (min); q_e (mg/g) is the amount of adsorbed Pb^{2+} ions at equilibrium; and K_1 (L/min) and K_2 (g/mg/min) are the rate constants for the first-order and second-order processes, respectively.

Two theoretical adsorption isotherm models were used to describe the equilibrium between the cell surfaces and Pb^{2+} ions: the Langmuir and Freundlich isotherm models [25]. The Langmuir model assumes that the adsorbent is a homogeneous surface with monolayer formation. In contrast, the Freundlich model isotherm describes adsorption occurring on heterogeneous surfaces with multilayered formation. The Langmuir isotherm model is described by Equation (5) [26]:

$$\frac{C_e}{q_e} = \frac{1}{Q_{max} K_L} + \frac{C_e}{Q_{max}} \quad (5)$$

where C_e (mg/L) is the equilibrium concentration of Pb^{2+} ions in aqueous solution; Q_{max} (mg/g) represents the maximum adsorption capacity; and K_L (L/mg) is the Langmuir adsorption constant.

The Freundlich model can be represented by Equation (6) [27]:

$$\text{Log}_{10}\, q_e = \log_{10} K_F + \log_{10}\, C_e \quad (6)$$

where K_F (L/g) is the Freundlich constant and n represents the affinity constant reflecting the strength of adsorption.

2.7. SEM–EDS, Fourier Transform Infrared (FTIR) and XRD Analysis

The cells before and after treatment with 200 mg/L Pb(II) solution were collected by centrifuging at 10,000 rpm for 15 min and were washed three times with deionized water. The samples were prepared for SEM–EDS and Fourier transform infrared (FTIR) analysis. The sample preparation steps of SEM–EDS were the same as those described before. Then, the cell morphology and elemental composition were analyzed by SEM–EDS. After being freeze-dried and mashed, the samples were analyzed by XRD and FTIR (Thermo Scientific, Waltham, MA, USA) to explore the functional groups that interacted with Pb^{2+} ions on the surfaces of PQ7.

2.8. Statistical Analysis

The experimental data were determined in triplicate and the mean values were calculated. The XRD and XPS data were analyzed by Jade 6.5 and Thermo Avantage, respectively. The pictures were drawn using OriginPro 2018 and Microsoft Excel, 2007.

3. Results and Discussion

3.1. Shinella Zoogloeoides PQ7 Turned Black in the Presence of Lead Ions

In the liquid medium with lead, we noticed that PQ7 cultures changed color from white to brown compared to the yellowish color on the blank controls. After cultivation for four days, the cells in vibrating liquid medium with Pb(II) turned eventually to black, a black precipitate was visible after centrifugation (Figure 1). The result indicated that PQ7 could produce a substance in the presence of lead ions. Many reports have shown that bacteria can produce nanoparticles with metal ions. For instance, biofilms of bacteria from the family *Desulfobacteriaceae* were found to produce ZnS nanoparticles [28]. In our study, we deduced that PQ7 might interact with lead ions in a similar way as *Desulfobacteriaceae*.

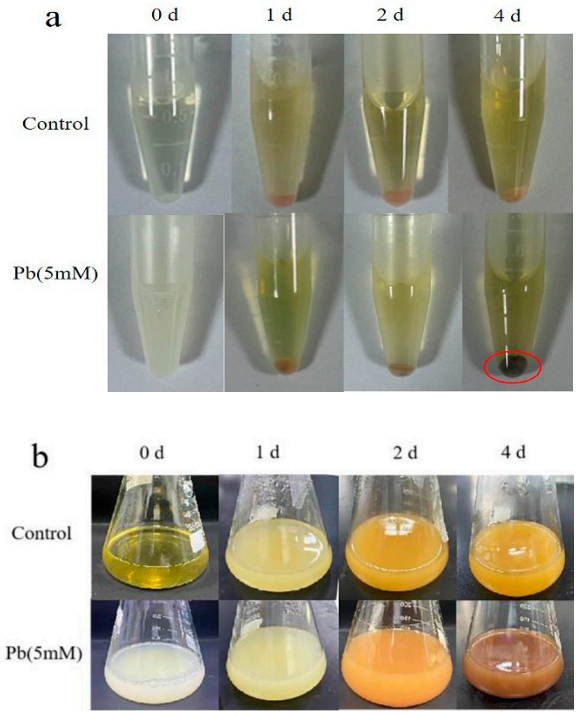

Figure 1. (**a**) The cells of PQ7 turn black in the presence of lead nitrate (5 mM). The red circle highlights the black precipitates. (**b**) The color change of PQ7 broth with or without lead nitrate (5 mM). The cells were cultivated at 30 °C with 200 rpm shaking speed. At the 4th day, the broth was brown with black precipitate after centrifugation.

3.2. PbS Nanoparticles Were Synthesized by PQ7

The TEM images indicated that nanoparticles were synthesized by *Shinella zoogloeoides* PQ7 in contrast to the control (Figure 2a,b). These nanoparticles were distributed outside the cells, and the size of the particles varied widely. It might be that small particles were synthesized and easily aggregated to form larger grains [29]. On the other hand, nanoparticles were also found around the cells in the liquid medium with Pb(II), according to the SEM images (Figure 2c). Based on the EDS elemental analyses, these areas were composed of C, N, P, S and Pb (Figure 2c).

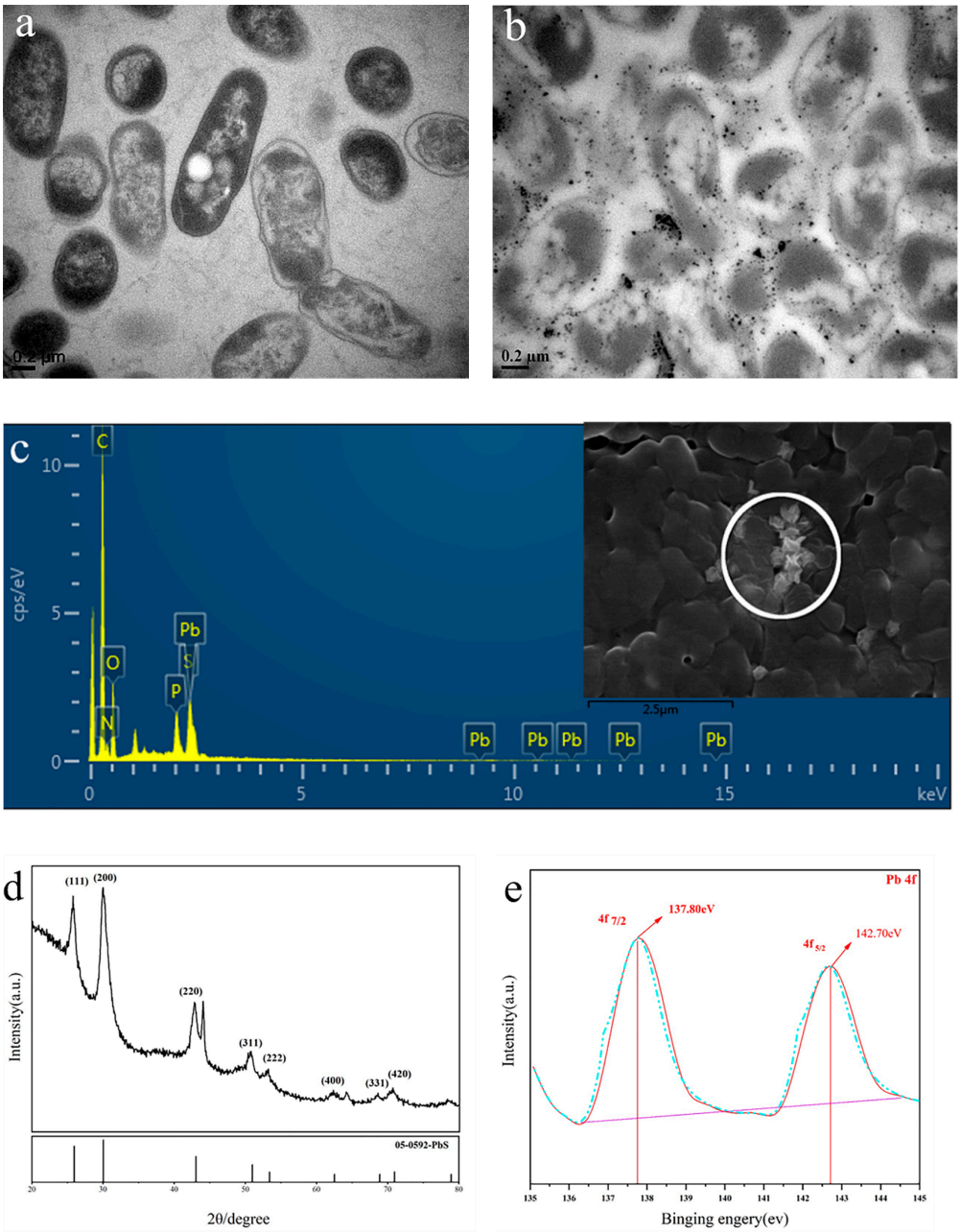

Figure 2. The characterization of the black materials synthesized by *Shinella zoogloeoides* PQ7. (**a**) Transmission electron microscope (TEM) image of control cells; (**b**) TEM image of cells with nanoparticles; (**c**) Scanning electron Microscopy–energy dispersive X-ray spectroscopy (SEM–EDS) of PQ7 grown with Pb (5 mM); (**d**) X-ray diffraction (XRD) pattern of PbS nanoparticles synthesized by PQ7; (**e**) X-ray photoelectron spectroscopy (XPS) image of PbS synthesized by PQ7.

The XRD result for black cells is shown in Figure 2d. From the image, it is clearly observed that the diffraction peaks at approximately 2θ = 25.96°, 30.07°, 43.05°, 50.97°, 53.41°, 62.53°, and 68.88° which correspond to the (111), (200), (220), (311), (222), (400) and (331) reflections, respectively. Based on comparison, these diffraction peaks can be matched with the presence of crystal PbS nanoparticles (according to Joint Committee on Powder Diffraction Standards (JCPDS) No: 05-0592) [30]. The result after fitting the original data by the software Avantage is shown in Figure 2e. Figure 2e displays only two Pb 4f peaks. The Pb 4f7/2 peak at 137.80 eV and Pb 4f5/2 peak at 142.70 eV were assigned to PbS [31]. The TEM, SEM–EDS, XRD and XPS data confirmed that PbS nanoparticles were biosynthesized by *Shinella zoogloeoides* PQ7.

Sulfate reduction in bacteria is an important mechanism for the formation of sulfide nanoparticles [32]. Sulfate ions are reduced to sulfur ions by this metabolic pathway. Under natural conditions, bacteria such as sulfate-reducing bacteria (SRB) can use reduced sulfur ions to produce hydrogen sulfide by combining with hydrogen ions. When metal ions are present, the hydrogen ions are replaced by metal ions to form insoluble metal sulfide [33,34]. The synthesis of PbS NPs in PQ7 might involve the same steps as described above. Although the synthesis of PbS NPs is not rare for microbes, this is the first report of PbS NPs synthesis by a strain in the genus *Shinella*.

3.3. Batch Biosorption Experiments

3.3.1. Effect of pH

The ability to synthesize PbS NPs suggests that PQ7 might attract lead ions from the environment. To fully explore its adsorption properties, some parameters, such as pH, contact time, biomass dosage and initial Pb(II) concentration, that influence the performance of adsorbents, were investigated. pH can impact the surface chemistry of bacteria to change the sorption efficiency [23]. The biosorption rate and capacity results with respect to pH values from 3.0 to 7.0 are depicted in Figure 3a. The biosorption rate and biosorption capacity both increased as the pH increased from 3 to 5. The maximum biosorption capacity and rate reached 134.22 mg/g and 67.11%, respectively, when the pH reached 5. Then, the rate and capacity of sorption declined when the pH changed from 5 to 7.

These results might be attributed to more carboxyl groups dissociating from the cell surface when the pH was 5, which enhanced the combination of Pb^{2+} ions with anionic ligands [35]. At pH 3 and 4, functional anionic active sites might be protonated on the cell surface, thus leaving many cationic groups in solution and limiting the biosorption rate and capacity of lead(II) [36]. When the solution is alkaline, precipitation might occur. The hydroxide ions (OH^-) in the solution could combine with lead ions (Pb^{2+}) to form precipitation ($Pb(OH)_2$). To distinguish adsorption from precipitation effectively, the pH should not be higher than 7 in adsorption experiments [37]. Therefore, pH 5 is an optimal condition for adsorption experiments of lead ions.

3.3.2. Effect of Contact Time

Figure 3b indicates the effect of contact time on the adsorption of Pb^{2+} ions by PQ7. In the first 60 min, the adsorption of lead ions was an extremely rapid process. After that, the process slowed and reached equilibrium at 90 min. In the equilibrium stage, the biological adsorption and rate reached 136.27 mg/g and 68.14%, respectively. In the adsorption of lead ions by bacteria, the first stage of the adsorption process of lead ions is the combination of the lead ions in solution with the functional groups in the microbial cell wall, which is fast, reversible and independent of energy metabolism [38]. In the later stage, lead is mainly precipitated or complexed, which is slow [39]. Therefore, the contact time of 90 min served as the most suitable equilibrium time.

3.3.3. Effect of Biosorbent Dosage

The influence of the biomass dosage was investigated by changing the adsorbent dosage from 0.5 g/L to 4.0 g/L. Figure 3c indicates that the biosorption rate increased from 27.48% to 97.99%

when the dosage changed from 0.5 g/L to 4.0 g/L. However, the maximum biosorption capacity of 134.21 mg/g was obtained at a dosage of 1 g/L. Moreover, the biosorption capacity declined rapidly as the biosorbent dosage increased from 1.0 g/L to 4.0 g/L. In the case of higher dosages of biological adsorbent, the available exchangeable sites on the cell surface could not be covered completely by the available solute, which led to a low capacity of adsorption. Moreover, the biosorption efficiency was also affected by competition for available metal ion adsorption sites and aggregation or overlapping on the cell surface [40]. Similar results were also indicated in previous studies [41,42]. In this study, 1.0 g/L was the ideal biomass dosage.

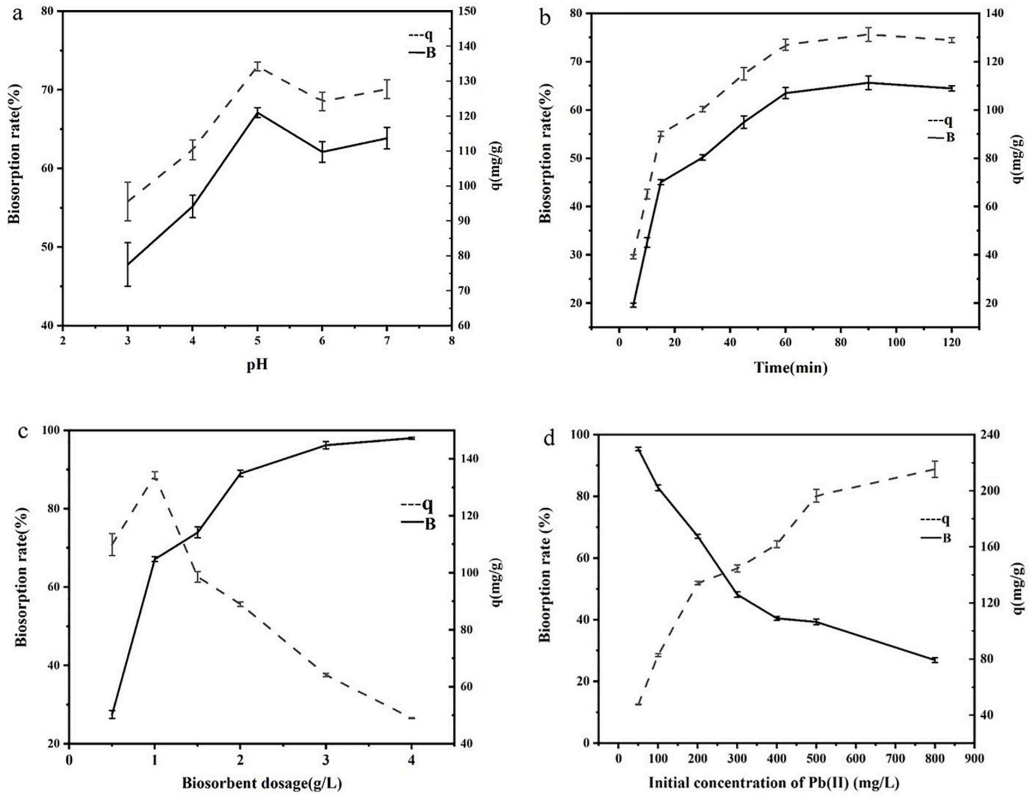

Figure 3. Some parameters influencing the performance of the adsorbent. (**a**) pH, (**b**) contact time, (**c**) biosorbent dosage and (**d**) initial Pb(II) concentration. The experimental conditions were as follows: (**a**) Pb(II) concentration = 200 mg/L, contact time = 90 min, biomass dosage = 1 g/L. (**b**) pH = 5, Pb(II) concentration = 200 mg/L, biomass dosage = 1 g/L. (**c**) pH = 5, contact time = 90 min, Pb(II) concentration = 200 mg/L. (**d**) pH = 5, biomass dosage = 1 g/L, contact time = 90 min. B and q indicate the biosorption rate (%) and biosorption capacity (mg/g), respectively. The values and error bars represent the means ± standard deviation (n = 3).

3.3.4. Effect of Initial Pb(II) Concentration

The adsorption efficiency and capacity can be affected immensely by the initial metal ion concentration [43]. A single-factor design was used to study the effect of different initial lead ion concentrations (50, 100, 200, 300, 400, 500 and 800 mg/L) at a contact time of 90 min, pH of 5, temperature of 30 °C, biomass dosage of 1 g/L and rotational speed of 200 rpm. As shown in Figure 3d, the sorption rate declined greatly from 95.35% to 26.93% when the initial concentration changed from 50 to 800 mg/L. Interestingly, the sorption capacity increased gradually as the initial concentration increased and reached 215.4 mg/g at a lead concentration of 800 mg/L. This result could be attributed to the solute molecules being less abundant than the effective surface sites at lower concentrations, leading to a much lower sorption capacity. In addition, as the initial concentration increased, the sites on the cell surface would become saturated, and the sorption capacity would become stable [44]. To balance

the sorption rate and capacity, 200 mg/L was chosen as a suitable initial concentration; at this value, the sorption rate and capacity were 67.1% and 134.2 mg/g, respectively.

3.4. Isotherm and Kinetic Modeling of the Biosorption of Pb(II)

The kinetics were studied to understand the mechanism of adsorption of lead ions. The experimental data were fitted by Equations (3) and (4) to evaluate the parameters of the pseudo-first order and pseudo-second order kinetic models. The data related to the kinetic models are indicated in Table 1 and Figure 4a. The correlation coefficient (R^2) of the pseudo-first-order kinetic model (0.962) was lower than that of the pseudo-second-order kinetic model (0.977). Moreover, the experimental data (q_{exp}) were closer to the data (q_{e2}) obtained from the pseudo-second-order kinetic model than those (q_{e1}) calculated from the pseudo-first-order model. This result meant that adsorption occurred not only on the cell surface but also through mass transfer via particle diffusion [45,46]. Thus, the adsorption of lead ions occurred through chemisorption [47].

To further understand the biosorption process of lead ions, the biosorption data were analyzed by the Langmuir and Freundlich isotherm models (Figure 4b,c). The parameters of these two isotherm models are shown in Table 1. From the table and figures, the correlation coefficient (R^2) of the Freundlich model (0.986) is better than that of the Langmuir model (0.978). This might be because the process of absorbing lead ions by PQ7 was based on adsorption on different surfaces and because the adsorption sites were not identical to or independent of each other, as reported in previous studies [21–23]. Table 2 compares the biosorption of Pb(II) by different bacteria. The maximum Pb(II) adsorption capacity of PQ7 was higher than those obtained in other reports. Thus, we deduced that the metal ion adsorption capacity of these microbes that could synthesize metal sulfide nanoparticles might be higher than that of some metal-resistant bacteria. This result may provide a direction for finding more efficient biosorbents. However, more experiments and data are needed to verify these results.

Table 1. Biosorption kinetic and adsorption isotherm parameters for the adsorption of Pb(II).

Pseudo-First-Order			**Pseudo-Second-Order**		
q_{e1} (mg/g)	K_1 (L/min)	R^2	q_{e2} (mg/g)	K_2 (g/mg/min)	R^2
130.98	0.065	0.962	139.91	0.000695	0.977
Langmuir Isotherm			**Freundlich Isotherm**		
Q_{max} (mg/g)	K_L (L/mg)	R^2	K_F (L/g)	n	R^2
222.22	0.022	0.978	38.49	3.65	0.986

Table 2. Comparative analysis of biosorbents for Pb(II) biosorption.

Bacteria	**q_{max} (mg/g)**	**Conditions**	**Reference**
Bacillus sp. ATS-1	92.3	pH 5, 25 °C	[48]
Geobacillus thermodenitrificans	32.26	pH 4.5, 35 °C	[49]
Pseudomonas aeruginosa PU21	110	pH 7, 37.5 °C	[48]
Alcaligenes sp. BAPb.1	66.7	pH 5, 30 °C	[35]
Bacillus cereus	36.7	pH 5.5, 30 °C	[50]
Pseudomonas fluorescens	77.6	pH 6, 30 °C	[51]
Bacillus pumilus	91.4	pH 6, 30 °C	[51]
Arthrobactor GQ-9	17.56	pH 5.5, 35 °C	[52]
Geobacillus thermodenitrificans	32.26	pH 4.5, 65 °C	[49]
Bacillus thioparans U3	210.1	pH 5, 30 °C	[25]
Alcaligenes sp.	56.8	pH 5, 35 °C	[35]
Bacillus sp. PZ-1	15.38	pH 5, 15 °C	[53]
Methylobacterium hispanicum EM2	79.84	pH 7, 30 °C	[21]
Pseudomonas stutzeri KCCM 34719	142	pH 6, 30 °C	[54]
Shinella zoogloeoides PQ7	222.22	pH 5, 30 °C	This study

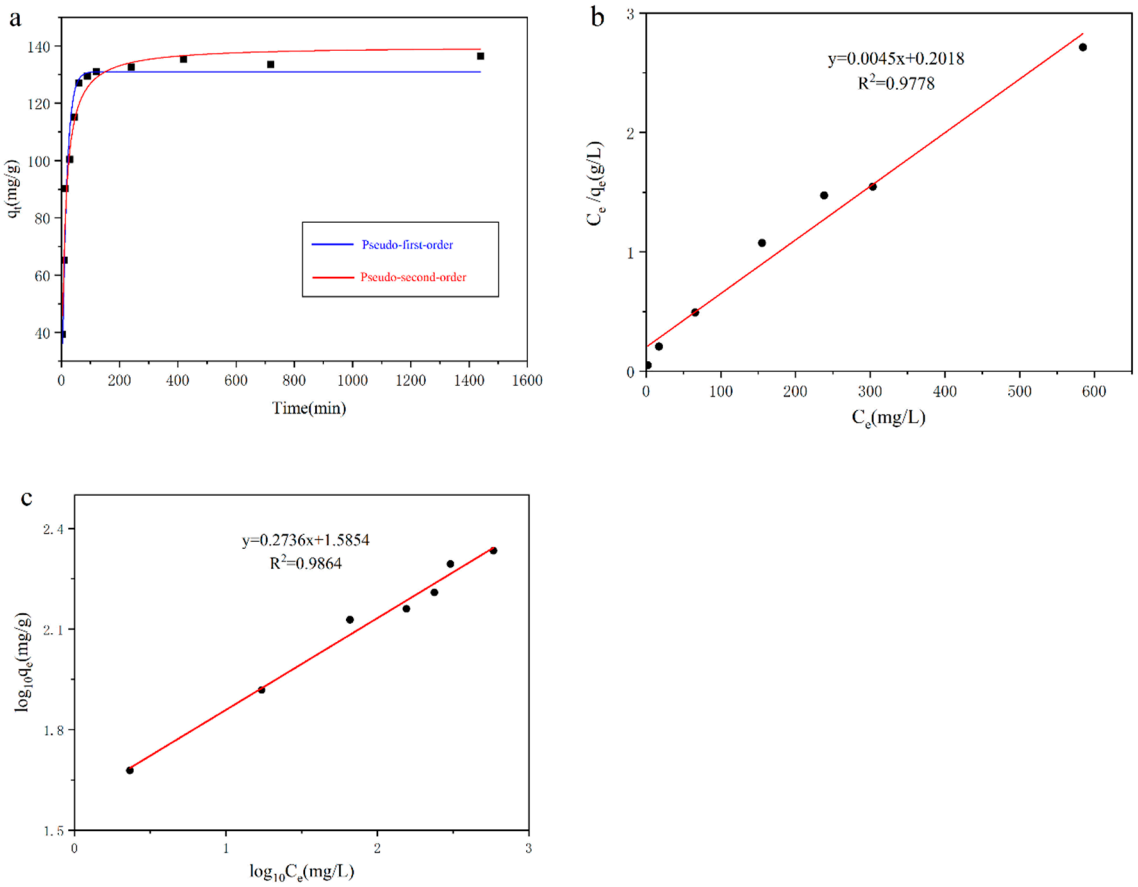

Figure 4. Isotherm and kinetic modeling of the biosorption of Pb(II). (**a**) Biosorption kinetic models; the blue line and red line represent the pseudo-first-order and pseudo-second-order models, respectively. Isotherms of Pb(II) biosorption by PQ7: (**b**) Langmuir; (**c**) Freundlich.

3.5. SEM–EDS, FTIR and XRD Analyses

It was observed from the SEM images that the morphology of the bacteria changed after treating with lead ions (Figure 5a,b). There were many protuberant particles on the cell surface after adsorption in comparison with the control (Figure 5a,b). The EDS data indicated that Pb(II) was present, and the atomic percentage (at%) was 1.65. The C and O (at%) contents decreased from 71.77 and 18.5 to 69.04 and 15.65, respectively, while the contents of N and P increased from 7.66 and 1.89 to 11.21 and 1.95, respectively, after treating lead ions (Figure 5a,b). These data indicated that C-, N-, P- and O-containing functional groups on the cell surface could combine with Pb(II). It has been reported that functional groups (amino, phosphate, carboxylate and hydroxyl) on the cell surface play an important role in the adsorption process [53,55,56].

FTIR spectra of bacteria before and after treatment with lead ions were obtained to investigate the interactions between Pb and the functional groups present on the cell walls. There were several changed absorption peaks due to the functional groups (Figure 5c). For example, the shift from 1541.77 cm^{-1} to 1534.87 cm^{-1} after treatment with Pb(II) corresponded to -NH vibrations [52]. The peak from 1395.72 cm^{-1} to 1391.18 cm^{-1} might be attributed to CO_3^{2-} stretching [57]. In addition, the peak at 1239.42 cm^{-1} (before contact with Pb(II)) shifted to 1234.42 cm^{-1} (after contact with Pb(II)), which was caused by C–O (carboxyl) stretching vibrations [58]. Moreover, the peak shift from 1082.91 cm^{-1} to 1061.24 cm^{-1} may be due to phosphate stretching vibrations in polysaccharides and nucleic acids [59]. The FTIR data analysis indicated that functional groups such as carboxyl, carbonyl and phosphate groups might participate in lead ion adsorption, which was also shown in the SEM–EDS data.

From the SEM image, Pb compounds might be synthesized on the cell surface after treatment with lead ions. Cells before and after the adsorption of Pb(II) were analyzed by XRD (Figure 5d). On the basis of matching with the standard cards of compounds in the Joint Committee on Powder Diffraction Standards (JCPDS) database, $Pb_5(PO_4)_3Cl$ (JCPDS-01-084-2045) and $Pb_{10}(PO_4)_6(OH)_2$ (JCPDS-01-087-2477) dominated the cell surface. The peaks of phosphate species were often observed at approximately 30 degrees. Phosphate is one of the important functional groups on the cell surface involved in the interaction between lead ions and cells and makes lead precipitate [60]. Therefore, the higher biosorption capacity of PQ7 might be attributed to the presence of many functional groups, such as phosphate and hydroxyl groups, on the bacterial surface that can induce the precipitation of Pb(II).

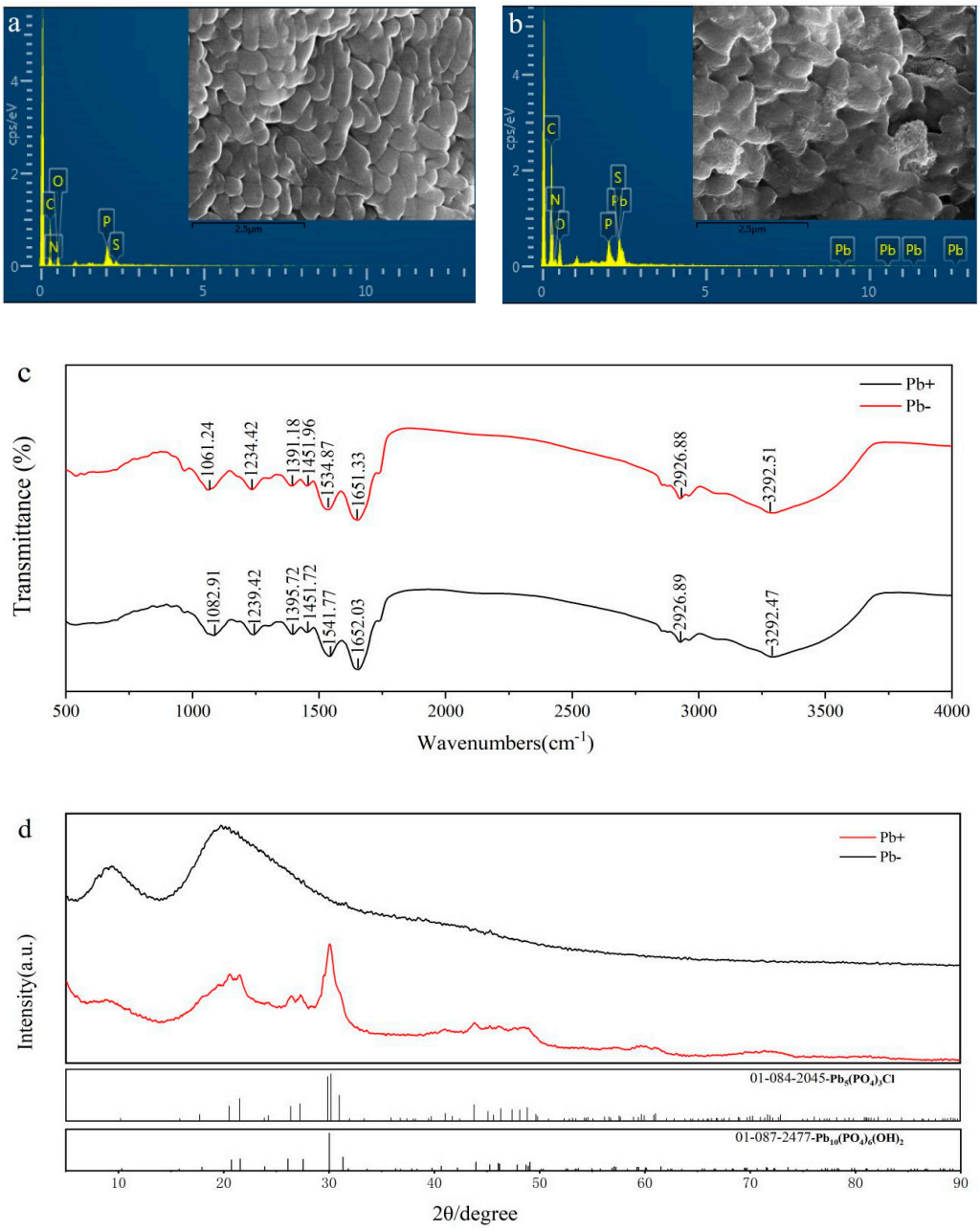

Figure 5. (**a**) and (**b**) were SEM–EDS spectra of PQ7 before and after treatment with lead ions, respectively; (**c**) FTIR and (**d**) XRD spectra of PQ7 before and after treatment with lead ions. The conditions were as follows: pH = 5, Pb(II) concentration = 200 mg/L, biomass = 1 g/L, contact time = 90 min.

4. Conclusions

In this study, we report that *Shinella zoogloeoides* PQ7 can synthesize PbS NPs in the presence of lead ions. Biosorption experiments with varying contact time, pH, biomass dosage and initial Pb(II) concentration were carried out to explore the adsorption behavior of Pb(II). The equilibrium data followed the Freundlich isotherm model, and the kinetic data fit well with the pseudo second-order model. The maximum (q_{max}) Pb(II) adsorption reached 222.22 mg/g, which was higher than that of other bacteria reported in previous literature. In summary, *Shinella zoogloeoides* PQ7 shows excellent potential for heavy metal bioremediation, and to remove Pb(II) from Pb(II)-contaminated wastewater.

Author Contributions: Conceptualization, W.Z. and Y.H.; methodology, W.Z.; investigation W.Z.; resources, Y.H.; data curation, W.Z.; writing—original draft preparation, W.Z.; writing—review and editing, W.Z. and Y.H.; visualization, W.Z.; supervision, Y.H.; funding acquisition, Y.H. All authors have read and agreed to the published version of the manuscript.

Funding: This work was financially supported by Chinese national key research and development plan [2017YFA0207003].

Conflicts of Interest: All authors declare that they have no conflict of interest.

References

1. Xiao, X.; Liu, Q.Y.; Lu, X.R.; Li, T.T.; Feng, X.L.; Li, Q.; Liu, Z.Y.; Feng, Y.J. Self-assembly of complex hollow CuS nano/micro shell by an electrochemically active bacterium *Shewanella oneidensis* MR-1. *Int. Biodeterior. Biodegrad.* **2017**, *116*, 10–16. [CrossRef]
2. Satapute, P.; Paidi, M.K.; Kurjogi, M.; Jogaiah, S. Physiological adaptation and spectral annotation of Arsenic and Cadmium heavy metal-resistant and susceptible strain *Pseudomonas taiwanensis*. *Environ. Pollut.* **2019**, *251*, 555–563. [CrossRef] [PubMed]
3. Sparks, D.L. Toxic metals in the environment: The role of surfaces. *Elements* **2005**, *1*, 193–197. [CrossRef]
4. Amaral, A.F.S.; Arruda, M.; Cabral, S.; Rodrigues, A.S. Essential and non-essential trace metals in scalp hair of men chronically exposed to volcanogenic metals in the Azores, Portugal. *Environ. Int.* **2008**, *34*, 1104–1108. [CrossRef] [PubMed]
5. Rana, S.V.S. Metals and apoptosis: Recent developments. *J. Trace Elem. Med. Biol.* **2008**, *22*, 262–284. [CrossRef]
6. Farooq, U.; Kozinski, J.A.; Khan, M.A.; Athar, M. Biosorption of heavy metal ions using wheat based biosorbents—A review of the recent literature. *Bioresour. Technol.* **2010**, *101*, 5043–5053. [CrossRef] [PubMed]
7. Zanardini, E.; Andreoni, V.; Borin, S.; Cappitelli, F.; Daffonchio, D.; Talotta, P.; Sorlini, C.; Ranalli, G.; Bruni, S.; Cariati, F. Lead-resistant microorganisms from red stains of marble of the Certosa of Pavia, Italy and use of nucleic acid-based techniques for their detection. *Int. Biodeterior. Biodegrad.* **1997**, *40*, 171–182. [CrossRef]
8. Templeton, A.S.; Trainor, T.P.; Spormann, A.M.; Newville, M.; Sutton, S.R.; Dohnalkova, A.; Gorby, Y.; Brown, G.E. Sorption versus biomineralization of Pb(II) within *Burkholderia cepacia* biofilms. *Environ. Sci. Technol.* **2003**, *37*, 300–307. [CrossRef]
9. Karnachuk, O.V.; Kurochkina, S.Y.; Tuovinen, O.H. Growth of sulfate-reducing bacteria with solid-phase electron acceptors. *Appl. Microbiol. Biotechnol.* **2002**, *58*, 482–486. [CrossRef]
10. Naik, M.M.; Pandey, A.; Dubey, S.K. *Pseudomonas aeruginosa* strain WI-1 from Mandovi estuary possesses metallothionein to alleviate lead toxicity and promotes plant growth. *Ecotox. Environ. Safe.* **2012**, *79*, 129–133. [CrossRef]
11. Seshadri, S.; Saranya, K.; Kowshik, M. Green Synthesis of Lead Sulfide Nanoparticles by the Lead Resistant Marine Yeast, *Rhodosporidium diobovatum*. *Biotechnol. Prog.* **2011**, *27*, 1464–1469. [CrossRef] [PubMed]
12. Priyanka, U.; Gowda, A.K.M.; Elisha, M.G.; Teja, S.B.; Nitish, N.; Mohan, R.B. Biologically synthesized PbS nanoparticles for the detection of arsenic in water. *Int. Biodeterior. Biodegrad.* **2017**, *119*, 78–86.
13. Kowshik, M.; Vogel, W.; Urban, J.; Kulkarni, S.K.; Paknikar, K.M. Microbial synthesis of semiconductor PbS nanocrystallites. *Adv. Mater.* **2002**, *14*, 815–818. [CrossRef]
14. Gong, J.; Zhang, Z.M.; Bai, H.J.; Yang, G.E. Microbiological synthesis of nanophase PbS by *Desulfotomaculum* sp. *Sci. China Ser. E-Technol. Sci.* **2007**, *50*, 302–307. [CrossRef]

15. Hosseini, M.R.; Sarvi, M.N. Recent achievements in the microbial synthesis of semiconductor metal sulfide nanoparticles. *Mater. Sci. Semicond. Process* **2015**, *40*, 293–301. [CrossRef]
16. Suganya, M.; Balu, A.R. PbS nanopowder—Synthesis, characterization and antimicrobial activity. *Mater. Sci.* **2017**, *35*, 322–328. [CrossRef]
17. Huang, Y.L.; Zeng, Y.H.; Yu, Z.L.; Zhang, J.; Feng, H.; Lin, X.C. In silico and experimental methods revealed highly diverse bacteria with quorum sensing and aromatics biodegradation systems—A potential broad application on bioremediation. *Bioresour. Technol.* **2013**, *148*, 311–316. [CrossRef]
18. Ma, Y.; Wei, Y.; Qiu, J.G.; Wen, R.T.; Hong, J.; Liu, W.P. Isolation, transposon mutagenesis, and characterization of the novel nicotine-degrading strain *Shinella* sp. HZN7. *Appl. Microbiol. Biotechnol.* **2014**, *98*, 2625–2636. [CrossRef]
19. Biala, S.; Chadha, P.; Saini, H.S. Biodegradation of 4-aminobenzenesulfonate by indigenous isolate *Shinella yambaruensis* SA1 and its validation by genotoxic analysis. *Biotechnol. Bioprocess Eng.* **2014**, *19*, 1034–1041. [CrossRef]
20. Wu, S.J.; Li, T.F.; Xia, X.; Zhou, Z.J.; Zheng, S.X.; Wang, G.J. Reduction of tellurite in *Shinella* sp. WSJ-2 and adsorption removal of multiple dyes and metals by biogenic tellurium nanorods. *Int. Biodeterior. Biodegrad.* **2019**, *144*, 10. [CrossRef]
21. Jeong, S.W.; Kim, H.K.; Yang, J.E.; Choi, Y.J. Removal of Pb(II) by Pellicle-Like Biofilm-Producing *Methylobacterium hispanicum* EM2 Strain from Aqueous Media. *Water* **2019**, *11*, 2081. [CrossRef]
22. Li, H.F.; Lin, Y.B.; Guan, W.M.; Chang, J.L.; Xu, L.; Guo, J.K.; Wei, G.H. Biosorption of Zn(II) by live and dead cells of *Streptomyces ciscaucasicus* Strain CCNWHX 72-14. *J. Hazard. Mater.* **2010**, *179*, 151–159. [CrossRef]
23. Yuvaraja, G.; Zheng, N.C.; Pang, Y.X.; Su, M.H.; Chen, D.Y.; Kong, L.J.; Mehmood, S.; Subbaiah, M.V.; Wen, J.C. Removal of U(VI) from aqueous and polluted water solutions using magnetic Arachis hypogaea leaves powder impregnated into chitosan macromolecule. *Int. J. Biol. Macromol.* **2020**, *148*, 887–897. [CrossRef] [PubMed]
24. Ho, Y.S.; McKay, G. Pseudo-second order model for sorption processes. *Process Biochem.* **1999**, *34*, 451–465. [CrossRef]
25. Rodriguez-Tirado, V.; Green-Ruiz, C.; Gomez-Gil, B. Cu and Pb biosorption on *Bacillus thioparans* strain U3 in aqueous solution: Kinetic and equilibrium studies. *Chem. Eng. J.* **2012**, *181*, 352–359. [CrossRef]
26. Langmuir, I. THE ADSORPTION OF GASES ON PLANE SURFACES OF GLASS, MICA AND PLATINUM. *J. Am. Chem. Soc.* **1918**, *40*, 1361–1403. [CrossRef]
27. Freundlich, H. Concerning adsorption in solutions. *Zeitschrift Fur Physikalische Chemie–Stochiometrie Und Verwandtschaftslehre* **1906**, *57*, 385–470.
28. Tanzil, A.H.; Sultana, S.T.; Saunders, S.R.; Shi, L.; Marsili, E.; Beyenal, H. Biological synthesis of nanoparticles in biofilms. *Enzyme Microb. Technol.* **2016**, *95*, 4–12. [CrossRef]
29. Bai, H.J.; Zhang, Z.M.; Guo, Y.; Yang, G.E. Biosynthesis of cadmium sulfide nanoparticles by photosynthetic bacteria *Rhodopseudomonas palustris*. *Colloid Surf. B-Biointerfaces* **2009**, *70*, 142–146. [CrossRef]
30. Shi, B.Z.; Qi, Y.; Tian, L.C.; Liu, L. The enhanced photoelectrochemical performance of PbS/ZnS quantum dots co-sensitized CdSe nanorods array heterostructure. *Mater. Sci. Semicond. Process* **2019**, *98*, 7–12. [CrossRef]
31. Ettema, A.; Haas, C. AN X-RAY PHOTOEMISSION SPECTROSCOPY STUDY OF INTERLAYER CHARGE-TRANSFER IN SOME MISFIT LAYER COMPOUNDS. *J. Phys.-Condes. Matter* **1993**, *5*, 3817–3826. [CrossRef]
32. Singh, R.; Kumar, A.; Kirrolia, A.; Kumar, R.; Yadav, N.; Bishnoi, N.R.; Lohchab, R.K. Removal of sulphate, COD and Cr(VI) in simulated and real wastewater by sulphate reducing bacteria enrichment in small bioreactor and FTIR study. *Bioresour. Technol.* **2011**, *102*, 677–682. [CrossRef]
33. Da Costa, J.P.; Girao, A.V.; Lourenco, J.P.; Monteiro, O.C.; Trindade, T.; Costa, M.C. Synthesis of nanocrystalline ZnS using biologically generated sulfide. *Hydrometallurgy* **2012**, *117*, 57–63. [CrossRef]
34. Li, X.; Lan, S.M.; Zhu, Z.P.; Zhang, C.; Zeng, G.M.; Livu, Y.G.; Cao, W.C.; Song, B.; Yang, H.; Wang, S.F.; et al. The bioenergetics mechanisms and applications of sulfate-reducing bacteria in remediation of pollutants in drainage: A review. *Ecotox. Environ. Safe.* **2018**, *158*, 162–170. [CrossRef] [PubMed]
35. Jin, Y.; Yu, S.M.; Teng, C.Y.; Song, T.; Dong, L.Y.; Liang, J.S.; Bai, X.; Xu, X.H.; Qu, J.J. Biosorption characteristic of *Alcaligenes* sp BAPb.1 for removal of lead(II) from aqueous solution. *3 Biotech* **2017**, *7*, 12. [CrossRef] [PubMed]

36. Rodriguez, C.E.; Quesada, A.; Rodriguez, E. Nickel biosorption by Acinetobacter baumannii and *Pseudomonas aeruginosa* isolated from industrial wastewater. *Braz. J. Microbiol.* **2006**, *37*, 465–467. [CrossRef]
37. Onundi, Y.B.; Mamun, A.A.; Al Khatib, M.F.; Ahmed, Y.M. Adsorption of copper, nickel and lead ions from synthetic semiconductor industrial wastewater by palm shell activated carbon. *Int. J. Environ. Sci. Technol.* **2010**, *7*, 751–758. [CrossRef]
38. Lan, T.; Ding, C.C.; Liao, J.L.; Li, X.L.; Li, X.L.; Zhang, J.; Zhang, D.; Yang, J.J.; Luo, S.Z.; An, Z.; et al. Biosorption behavior and mechanism of thorium on *Bacillus* sp dwc-2 isolated from soil. *Nucl. Sci. Tech.* **2015**, *26*, 11.
39. Yetis, U.; Ozcengiz, G.; Dilek, F.B.; Ergen, N.; Dolek, A. Heavy metal biosorption by white-rot fungi. *Water Sci. Technol.* **1998**, *38*, 323–330. [CrossRef]
40. El-Sayed, M.T. Removal of lead(II) by *Saccharomyces cerevisiae* AUMC 3875. *Ann. Microbiol.* **2013**, *63*, 1459–1470. [CrossRef]
41. Masoudzadeh, N.; Zakeri, F.; Lotfabad, T.B.; Sharafi, H.; Masoomi, F.; Zahiri, H.S.; Ahmadian, G.; Noghabi, K.A. Biosorption of cadmium by *Brevundimonas* sp ZF12 strain, a novel biosorbent isolated from hot-spring waters in high background radiation areas. *J. Hazard. Mater.* **2011**, *197*, 190–198. [CrossRef] [PubMed]
42. Khadivinia, E.; Sharafi, H.; Hadi, F.; Zahiri, H.S.; Modiri, S.; Tohidi, A.; Mousavi, A.; Salmanian, A.H.; Noghabi, K.A. Cadmium biosorption by a glyphosate-degrading bacterium, a novel biosorbent isolated from pesticide-contaminated agricultural soils. *J. Ind. Eng. Chem.* **2014**, *20*, 4304–4310. [CrossRef]
43. SalehA, T.A.; Gupta, V.K.; Al-Saadi, A.A. Adsorption of lead ions from aqueous solution using porous carbon derived from rubber tires: Experimental and computational study. *J. Colloid Interface Sci.* **2013**, *396*, 264–269. [CrossRef] [PubMed]
44. Vijayaraghavan, K.; Yun, Y.S. Bacterial biosorbents and biosorption. *Biotechnol. Adv.* **2008**, *26*, 266–291. [CrossRef] [PubMed]
45. Sobhanardakani, S.; Jafari, A.; Zandipak, R.; Meidanchi, A. Removal of heavy metal (Hg(II) and Cr(VI)) ions from aqueous solutions using Fe_2O_3@SiO_2 thin films as a novel adsorbent. *Process Saf. Environ. Protect.* **2018**, *120*, 348–357. [CrossRef]
46. Rodrigues, E.; Almeida, O.; Brasil, H.; Moraes, D.; dos Reis, M.A.L. Adsorption of chromium (VI) on hydrotalcite-hydroxyapatite material doped with carbon nanotubes: Equilibrium, kinetic and thermodynamic study. *Appl. Clay Sci.* **2019**, *172*, 57–64. [CrossRef]
47. Zafar, M.N.; Nadeem, R.; Hanif, M.A. Biosorption of nickel from protonated rice bran. *J. Hazard. Mater.* **2007**, *143*, 478–485. [CrossRef]
48. Tunali, S.; Cabuk, A.; Akar, T. Removal of lead and copper ions from aqueous solutions by bacterial strain isolated from soil. *Chem. Eng. J.* **2006**, *115*, 203–211. [CrossRef]
49. Chatterjee, S.K.; Bhattacharjee, I.; Chandra, G. Biosorption of heavy metals from industrial waste water by *Geobacillus thermodenitrificans*. *J. Hazard. Mater.* **2010**, *175*, 117–125. [CrossRef]
50. Pan, J.H.; Liu, R.X.; Tang, H.X. Surface reaction of Bacillus cereus biomass and its biosorption for lead and copper ions. *J. Environ. Sci.* **2007**, *19*, 403–408. [CrossRef]
51. Wierzba, S.; Latala, A. Biosorption lead(II) and nikel(II) from an aqueous solution by bacterial biomass. *Pol. J. Chem. Technol.* **2010**, *12*, 72–78. [CrossRef]
52. Wang, T.Q.; Yao, J.; Yuan, Z.M.; Zhao, Y.; Wang, F.; Chen, H.L. Isolation of lead-resistant *Arthrobactor* strain GQ-9 and its biosorption mechanism. *Environ. Sci. Pollut. Res.* **2018**, *25*, 3527–3538. [CrossRef] [PubMed]
53. Ren, G.M.; Jin, Y.; Zhang, C.M.; Gu, H.D.; Qu, J.J. Characteristics of *Bacillus* sp PZ-1 and its biosorption to Pb(II). *Ecotox. Environ. Safe.* **2015**, *117*, 141–148. [CrossRef] [PubMed]
54. Gupta, V.K.; Rastogi, A. Biosorption of lead from aqueous solutions by green algae *Spirogyra* species: Kinetics and equilibrium studies. *J. Hazard. Mater.* **2008**, *152*, 407–414. [CrossRef] [PubMed]
55. Lim, M.S.; Yeo, I.W.; Roh, Y.; Lee, K.K.; Jung, M.C. Arsenic reduction and precipitation by *shewanella* sp.: Batch and column tests. *Geosci. J.* **2008**, *12*, 151–157. [CrossRef]
56. Monteiro, C.M.; Castro, P.M.L.; Malcata, F.X. Biosorption of zinc ions from aqueous solution by the microalga *Scenedesmus obliquus*. *Environ. Chem. Lett.* **2011**, *9*, 169–176. [CrossRef]

57. Cai, Y.; Li, X.P.; Liu, D.Y.; Xu, C.L.; Ai, Y.W.; Sun, X.M.; Zhang, M.; Gao, Y.; Zhang, Y.C.; Yang, T.; et al. A Novel Pb-Resistant *Bacillus subtilis* Bacterium Isolate for Co-Biosorption of Hazardous Sb(III) and Pb(II): Thermodynamics and Application Strategy. *Int. J. Environ. Res. Public Health* **2018**, *15*, 702. [CrossRef] [PubMed]
58. Aravindhan, R.; Madhan, B.; Rao, J.R.; Nair, B.U.; Ramasami, T. Bioaccumulation of chromium from tannery wastewater: An approach for chrome recovery and reuse. *Environ. Sci. Technol.* **2004**, *38*, 300–306. [CrossRef]
59. Rodriguez-Sanchez, V.; Guzman-Moreno, J.; Rodriguez-Gonzalez, V.; Flores-de La Torre, J.; Ramirez-Santoyo, R.M.; Vidales-Rodriguez, L.E. Biosorption of lead phosphates by lead-tolerant bacteria as a mechanism for lead immobilization. *World J. Microbiol. Biotechnol.* **2017**, *33*, 11. [CrossRef]
60. Huang, J.; Huang, Z.L.; Zhou, J.X.; Li, C.Z.; Yang, Z.H.; Ruan, M.; Li, H.; Zhang, X.; Wu, Z.J.; Qin, X.L.; et al. Enhancement of heavy metals removal by microbial flocculant produced by *Paenibacillus polymyxa* combined with an insufficient hydroxide precipitation. *Chem. Eng. J.* **2019**, *374*, 880–894. [CrossRef]